Available online at www.sciencedirect.com
SCIENCE DIRECT
Journal of Photochemistry and Photobiology A: Chemistry 176 (2005) 191–198
Journal of Photochemistry and Photobiology A:Chemistry
www.elsevier.com/locate/jphotochem

Nascent vibrational distributions and relaxation rates of diatomic products of the reactions of $O(^1D)$ with CH_4, C_2H_6, CH_3F, CH_2F_2 and CHF_3 studied by time resolved Fourier transform infrared emission

Gus Hancock *, Marc Morrison, Mark Saunders

Physical and Theoretical Chemistry Laboratory, Oxford University, South Parks Road, Oxford OX1 3QZ, UK

Received 18 July 2005; received in revised form 2 September 2005; accepted 10 October 2005

Abstract

Time resolved Fourier transform infrared (TRFTIR) emission has been used to study the reactions of CH_4, C_2H_6, CH_3F, CH_2F_2 and CHF_3 with $O(^1D)$. One hundred and ninety-three nanomters photolysis of N_2O was used to prepare $O(^1D)$, and emission analysed from $OH(\nu = 1–4)$ for the two hydrocarbons and $HF(\nu = 1–6)$ from CH_3F, CH_2F_2 and CHF_3. For the $O(^1D) + CH_4$ reaction, the nascent OH vibrational distribution showed a population inversion between $\nu = 1$ and 2, and was in excellent agreement with previous laser induced fluorescence and TRFTIR data, as well as with quasi-classical trajectory calculations. Time resolved populations were analysed to yield rate constants for vibrational relaxation of $OH(\nu)$ with CH_4, and found to be consistent with stepwise deexcitation rather than chemical removal being dominant. Reaction with C_2H_6 produced a monotonically decreasing population in $\nu = 1–4$ and more rapid relaxation rates than those with methane. For the fluorinated methanes, nascent vibrational populations in $HF(\nu = 1–6)$ were measured and shown to be very similar, all monotonically decreasing with ν, and fitting the same vibrational surprisal plot, showing a larger than statistical partitioning of the available energy in vibration. Relaxation rate constants of $HF(\nu)$ with the parent fluorinated methane showed values, which increased with increasing H atom content.

Keywords: Laser; Infrared; FTIR; Fluorocarbons; $O(^1D)$

1. Introduction

The gas phase removal processes of electronically excited $O(^1D)$ atoms in potentially reactive collisions with methane CH_4 and fluorinated methanes of the form CH_nF_{4-n} where $n = 1–3$ show several common characteristics. First they are all fast, having rate constants which are close to gas kinetic values for CH_4 and CH_3F of 1.5×10^{-10} and 1.6×10^{-10} cm^3 $molecules^{-1}$ s^{-1}, respectively, and falling with increasing F atom content to a value of 10^{-11} cm^3 $molecule^{-1}$ s^{-1} for CHF_3 [1]. Secondly, they have the possibility of multiple channels in the reaction products as well as contributions from physical quenching to the $O(^3P)$ ground state. For CH_4, the major channel is to form OH [2–4] and quenching is negligible. For the fluorinated species, HF is always found as a major reaction product, and the proportion of collisions leading to quenching increases with F atom content [5–8]. The reactions forming these diatomic products are all highly exothermic, and can form vibrationally excited species. For the process

$$O(^1D) + CH_4 \rightarrow CH_3 + OH(\nu) \quad (1)$$

vibrational levels up to $\nu = 4$ are thermodynamically possible, and levels up to the thermodynamic limit have been observed in previous studies [2,9,10]. For HF formation in conjunction with the appropriate formaldehyde co-product

$$O(^1D) + CH_nF_{4-n} \rightarrow CH_{n-1}F_{3-n}O + HF(\nu) \quad (2)$$

the exothermicities lie in the range 582–642 kJ mol^{-1}, exceeding the HF dissociation energy and thus allowing populations in all vibrational levels of HF. Previous work on the CHF_3 reaction has identified levels up to $\nu = 6$ [6,11] and for the other two fluorinated methanes vibrational excitation up to $\nu = 3$ has been observed [11].

In this paper, we describe TRFTIR measurements of the products of reactions of $O(^1D)$. We observe the nascent vibrational distribution of OH in the reaction of $O(^1D)$ with methane,

* Corresponding author. Tel.: +44 1865 275400/275439; fax: +44 1865 275410.
E-mail address: gus.hancock@chem.ox.ac.uk (G. Hancock).

1010-6030/$ – see front matter © 2005 Elsevier B.V. All rights reserved.
doi:10.1016/j.jphotochem.2005.10.006

reaction (1), and also with ethane

$$O(^1D) + C_2H_6 \rightarrow C_2H_5 + OH(\nu) \quad (3)$$

and determine the rates of loss of vibrational energy from OH(ν) in collisions with the parent molecule. Vibrational populations of OH in reactions (1) and (3) have been previously measured by laser-induced fluorescence (LIF) [9,10,12] as well by TRFTIR for reaction (1) [2]. Although LIF has higher sensitivity than TRFTIR, the advantage of the latter technique is that all vibrationally excited levels can be observed simultaneously, and this removes the necessity for correction of the observed LIF signals for the different wavelengths of excitation and emission which accompany measurements on a wide variety of vibrational states. For the OH nascent distributions, we compare our results with previous work [2,9,10,12]. Our observations of OH removal rates have been analysed both in terms of a single quantum cascade mechanism and with allowance for reactive removal of OH, with the former providing more consistent comparison with previous data [9,13–16]. We also observe TRFTIR emission from the HF product of reaction (2) for each of the three-fluorinated methanes. We compare our data with previous nascent populations, either measured by the TRFTIR [2] or by laser gain [11,17] and we obtain a complete set of self quenching data which show rate constants which increase monotonically with H atom content of the fluorinated methane.

2. Experimental

The major features of the TRFTIR apparatus have been described previously [18,19] and are summarised here. $O(^1D)$ was produced by the 193 nm photolysis of N_2O in the presence of the reactant and generally an excess of Ar to ensure that rotational (but not vibrational) thermalisation of the OH or HF product was complete on the time scale of the observations. Emission was observed with a Welsh cell arrangement, passed through a FTIR spectrometer operating in the step scan mode (Bruker FS 66/S) and the resultant signal observed normally with 1 μs resolution over a time period typically 200 μs and averaged over 20 laser shots, with signal levels normalised for laser intensity fluctuations. The data consist of time resolved emission as a function of interferometer path difference, and the resultant time resolved interferograms are converted to time resolved emission spectra by fast Fourier transform.

Reagent purities were as follows: N_2O (BOC) > 99.997%, C_2H_6 (BOC) > 99%, CH_4 (BOC) > 99.5%, CH_3F (Lancaster) > 99%, CH_2F_2 (Fluorochem) > 99.7%, CHF_3 (Aldrich) 98%. Total pressures were measured with capacitance manometers (Datametrics Barocell 600 A 10 Torr Head, MKS Batratron 122-AA 1000 Torr head) and converted to partial pressures through measured flow rates through the reaction vessel. All measurements were carried out at room temperature, 295 K.

3. Results and discussion

Our previous TRFTIR emission studies of the 193 nm photolysis of N_2O [19] have shown that infrared emission can be seen from NO (ν) in both the fundamental ($\Delta\nu = -1$) transitions between 1600 and 1900 cm^{-1} for $\nu = 1$–14 and the first overtone ($\Delta\nu = -2$) transitions between 3400 and 3700 cm^{-1} for $\nu = 2$–14 and arising from the reaction of the $O(^1D)$ photofragment with the parent molecule

$$O(^1D) + N_2O \rightarrow 2NO \quad (4)$$

In addition strong emission from the $N_2O(\Delta\nu_3 = -1)$ transitions is seen near 2200 cm^{-1}, the vibrationally excited molecule being formed from energy transfer from the internally excited N_2 cofragment of N_2O photolysis [19]. Hydrocarbon reagents were always added in excess such that reactions (1–3) dominated over (4) for removal of $O(^1D)$ and thus fundamental emissions from OH (observed between 3000 and 3800 cm^{-1}) or HF (2500–4200 cm^{-1}) were not markedly affected by that from NO.

$O(^1D) + CH_4$

The major step in the reaction of $O(^1D)$ with methane is to form the OH radical, accounting for some 70–80% of $O(^1D)$ removal [2–4,20] and the removal rate constant is fast, the recommended value being 1.5×10^{-10} cm^3 $molecule^{-1}$ s^{-1}. Fig. 1 shows a time slice of the fundamental emission region from OH recorded from the $O(^1D) + CH_4$ reaction.

Marked on the figure are the positions of the Q-branches for the ($\Delta\nu = -1$) transitions originating in $\nu = 1$–4, and a simulation is shown which represents the best-fit to a 295 K rotational distribution with the vibrational populations treated as adjustable parameters. Spectral simulations used the *J* dependent transition probabilities calculated by Turnbull and Lowe [21]. The relative populations of vibrational levels 1–4 were extracted at 1 μs intervals and extrapolated to zero time to obtain nascent populations

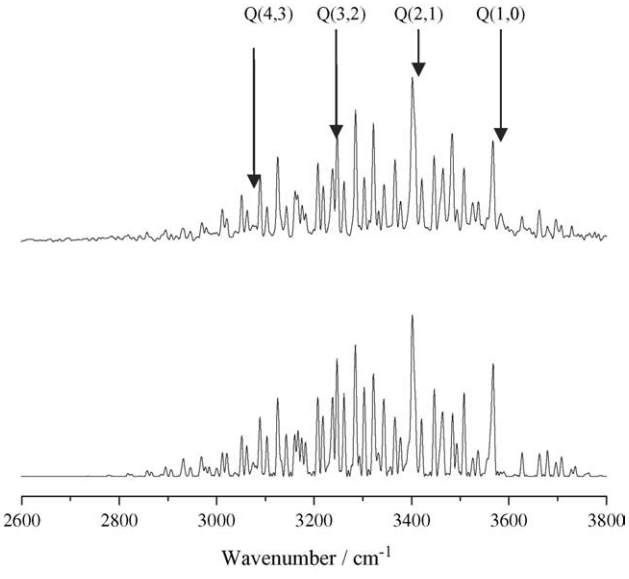

Fig. 1. OH($\Delta\nu = -1$) emission spectrum (upper trace) from $O(^1D) + CH_4$; $p(N_2O) = 200$ m Torr, $p(CH_4) = 500$ m Torr, $t = 10$ μs. Also shown as the lower trace and offset on the vertical scale for clarity is the best-fit OH($\Delta\nu = -1$) simulation for a rotational temperature of 295 K with vibrational populations for $\nu = 1$–4 as the adjustable parameters. The Q-branches of OH($\nu = 1$–4) are marked at 3565, 3400, 3240 and 3080 cm^{-1}, respectively (resolution = 4 cm^{-1}).

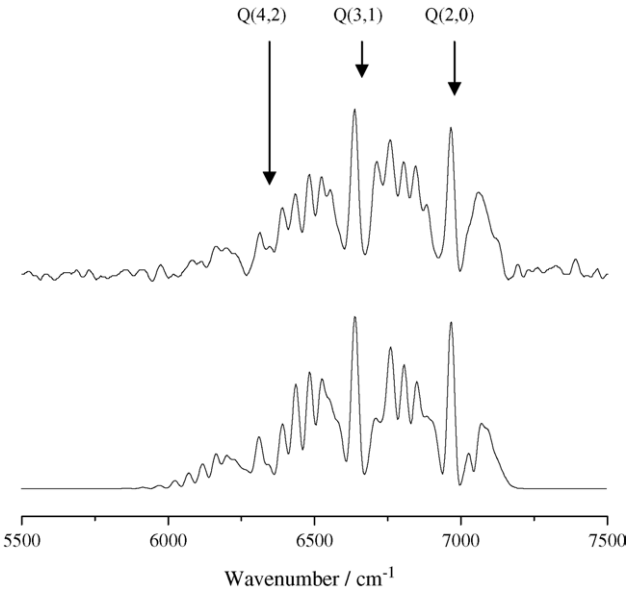

Fig. 2. OH($\Delta\nu = -2$) emission (upper trace) from the $O^1D + CH_4$ reaction; $p(N_2O) = 250$ m Torr, $p(CH_4) = 750$ m Torr, $t = 5$–15 μs. The best-fit OH($\Delta\nu = -2$) simulation (lower trace) is offset from the data as in Fig. 1. Q-branch heads from $\nu = 2$, 3 and 4 can again be seen at 6974, 6644 and 6318 cm^{-1}, respectively, and are marked on the figure (resolution 20 = cm^{-1}).

as described previously for measurements of the vibrational populations of NO in the dissociation of NO_2 [18,22]. Spectra were also recorded in the weaker OH first overtone region near 6600 cm^{-1}, and an example is shown in Fig. 2.

Extraction of populations in levels $\nu = 2$–4 was carried out as for the fundamental data. Table 1 shows the fractional populations of the vibrationally excited states, taken as weighted averages over the nascent distributions measured over a pressure range of 0.25–1 Torr of CH_4 for 5 sets of measurements on the fundamental and 5 on the overtone, and the results are plotted in Fig. 3.

Table 1 and Fig. 3 also show the results of three previous investigations, one by TRFTIR emission as in this study [2], and two previous LIF measurements [9,10]. The present results are in almost exact agreement with the previous TRFTIR work [2], and both of these sets of results show a higher degree of vibrational excitation compared with the LIF data [9,10], and this is shown in the relatively higher populations observed in $\nu = 3$ and 4 by emission in comparison with LIF. Criticism [10] has been directed towards one [9] of the LIF studies for the use of $\Delta\nu = 0$ transitions in excitation of the A–X band of OH. Here there is the possibility of underestimating the population in $\nu = 2$–4 because of predissociation in the upper A state, and this may account for the vanishingly low population reported [9] in $\nu = 4$ in one of these studies.

Table 1
Relative populations: OH nascent vibrational distribution from the reaction $O(^1D) + CH_4$

ν	This work	[2]	[9]	[10]
0	–	–	0.22	0.32
1	0.24 ± 0.03	0.27 ± 0.04	0.35	0.33
2	0.33 ± 0.02	0.33 ± 0.03	0.45	0.43
3	0.26 ± 0.02	0.26 ± 0.04	0.18	0.17
4	0.17 ± 0.03	0.14 ± 0.03	0.01	0.07

Errors are shown where appropriate as $\pm 1\sigma$. Also included are previously reported measurements by TRFTIR emission [2] and LIF [9,10]. All data are summed to unity for the vibrationally excited levels. In references [2,9,10] $O(^1D)$ was formed from the 248/266 nm photolysis of ozone.

We now comment on two further points. First, the 193 nm photolysis of N_2O produces $O(^1D)$ with an average kinetic energy of 0.74 eV [23]. We observe no effect within experimental error on the nascent vibrational populations in experiments carried out over a range of pressures and also in the presence or absence of Ar. This implies that, within our experimental error, either the vibrational distribution is insensitive to translational excitation, or that thermalisation of the nascent $O(^1D)$ is taking place in competition with reaction: translational relaxation of $O(^1D)$ has a rate constant [24] similar to that for removal by reaction with N_2O [25], and thus significant thermalisation would occur in the presence of Ar at typical pressures used (ca. 5 Torr). We note that the experiments with which we compare our data [2,9,10] were carried out with $O(^1D)$ formed from the 248/266 nm photolysis of ozone, and hence with a lower kinetic energy than the nascent $O(^1D)$ from the 193 nm photolysis of N_2O. We are unable to quantify the effects of translational energy on the vibrational distributions, however, because of the thermalisation induced in the present experiments. Quasi-classical trajectory (QCT) calculations of Gonzalez et al. [12,26] show that the effect of translational excitation is to open up small populations in levels above the room temperature thermodynamic limit of $\nu = 4$, and also to remove the population inversion seen at low collision energies between levels $\nu = 0$, 1 and 2. The QCT calculations for the lowest collision energy studied [12], 0.212 eV, are plotted in Fig. 3 and show almost exact agreement with both the first TRFTIR study of this reaction [2] and our present data. More recent calculations on an improved PES and for a nascent $O(^1D)$ velocity distribution appropriate to that formed from 193 nm photolysis of N_2O show similar values [27]. Secondly, our results apply to rotationally thermalised OH. Spectra taken at total pressures less than 500 m Torr revealed a high degree of rotational excitation at early times, but nascent rotational conditions could not be achieved, and the best-fit estimate

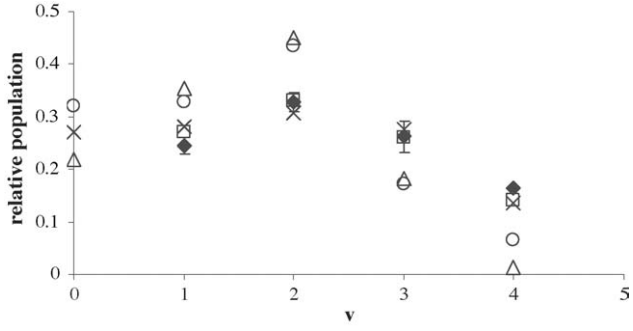

Fig. 3. Relative OH populations: comparison of this work (filled diamonds) with those of Aker et al. [2] (squares) Cheskis et al. [9] (triangles) and Park and Wiesenfeld [10] (circles). Populations are summed to unity for $\nu > 0$. The crosses show the quasi-classical trajectory calculations of Gonzalez et al. [12] carried out at a collision energy of 0.212 eV.

of a rotational distribution produced a rotational temperature of 1500–2000 K after approximately 10 gas kinetic collisions. LIF is a far superior technique for measuring rotational distributions, and previous work has shown populations extending to states up to the thermochemical threshold and consistent with our qualitative observations of high rotational excitation [9,10,28,29]. The measurements of such rotational excitation coupled with a partially inverted vibrational distribution have been explained in terms of insertion of the $O(^1D)$ in the C–H bond, followed by dissociation of the intermediate complex with both prompt and slow OH elimination [10,26–28,30–35].

The analysis of the time resolved populations can be used to determine collisional relaxation rates into and out of the measured levels providing that a suitable model for the relaxation processes is assumed. There are two limiting cases, namely stepwise quantum loss, of the form

$$OH(\nu) + CH_4 \rightarrow OH(\nu - 1) + CH_4 \quad (5)$$

where CH_4 is most likely to be formed in the ν_3 mode, a process which is close to resonance for $\nu = 4$ of OH, or complete removal of vibrational energy so that it is subsequently unobserved in emission, for example by reactive removal or by redissociation of an OH–CH_4 complex preferentially into OH $\nu = 0$. Experimentally we observe that lower vibrational levels peak at later times, indicative of a substantial contribution from process (5), and we now describe efforts to fit the data to various models.

First we consider purely stepwise relaxation. We show in Fig. 4 an example of the fitting of a stepwise model (i.e. with only processes (5) for removal of OH in collisions with CH_4) to the data for $\nu = 1$ at a given pressure of CH_4. Fig. 5 shows relaxation rates extracted for this model as a function of CH_4 pressure, with the resultant rate constants shown in Table 2. The Table also shows previously reported values of removal of OH(ν) by CH_4 [9,13–16,36,37].

We note that our data for the highest level measured, $\nu = 4$, should be independent of whether we choose exclusive or partial stepwise loss of quanta, but that differences would be expected when we analyse for the behaviour of the lower levels, particularly for $\nu = 1$. As can be seen from Table 2, pure stepwise relaxation gives a rate constant for $\nu = 1$ in good agreement with all previous measurements, which have used various methods for OH(ν) production, including the $O(^1D) + CH_4$ reaction [9,14,37] the $H + NO_2$ reaction [36], and also clean formation of a single vibrational level, $\nu = 2$, by overtone pumping [13,16]. In the latter case, cascade into $\nu = 2$ is avoided and the observed rate constant

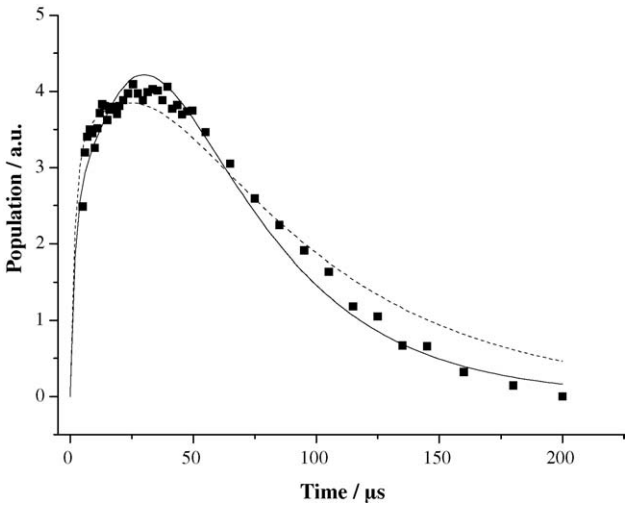

Fig. 4. Temporal profile of OH($\nu = 1$) following the reaction $O(^1D) + CH_4$; $p(N_2O) = 250$ m Torr, $p(CH_4) = 500$ m Torr. Also shown are the fits to the data from the two kinetic models used: the single quantum cascade mechanism (solid line) and the same mechanism with the introduction of 40% reactive removal (dashed line) as described in the text.

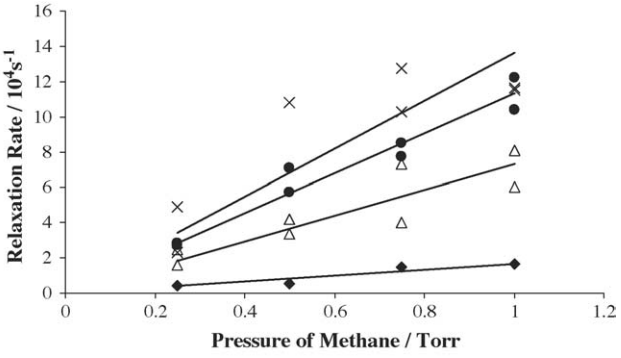

Fig. 5. Relaxation rates of OH($\nu = 1$–4) by CH_4, determined from fits of the model to time-dependent vibrational population data: $\nu = 1$ (filled diamonds) $\nu = 2$ (triangles) $\nu = 3$ (filled circles) $\nu = 4$ (crosses). The solid lines represent the linear fits to the data that reveal the rate of relaxation for each ν.

for the loss of this level is identical to the present value, suggesting that our results appear consistent with a stepwise mechanism. The rate constants increase with vibrational excitation, in a manner consistent with the change in energy discrepancy in process (5) if CH_4 is excited in the ν_3 mode, also shown in Table 2.

However, the stepwise mechanism has been called into question. One of the LIF studies carried out on the products of

Table 2
OH($\nu = 1$–4) vibrational relaxation rate constants (in units of 10^{-12} cm^3 molecule^{-1} s^{-1}) in collisions with methane together with previously reported values

ν	ΔE (cm^{-1})	This work (a)	40% reactive removal (b)	[9]	[13]	[14]	[15]	[16]	[36]	[37]
1	−546	0.57 ± 0.05	0.38 ± 0.04	0.51	0.50	0.51	0.53	–	2.10	0.56
2	−381	2.16 ± 0.35	1.93 ± 0.25	1.50	2.50	2.00	1.30	2.30	5.00	2.00
3	−221	3.67 ± 0.23	3.16 ± 0.22	6.80	–	4.50	–	–	–	4.80
4	−61	4.92 ± 1.03	4.53 ± 0.91	–	–	–	–	–	–	8.60

The first column of experimental data (a), from this work, is for analysis of the data by stepwise relaxation; and the second column (b) for a reactive component comprising 40% of the total removal rate. Errors are shown as $\pm 1\sigma$. Also presented are the energy discrepancies for the V–V exchange process in which one quantum loss of energy in OH is accompanied by excitation of one quantum in the $CH_4(\nu_3)$ mode. The measurements reported in [37] have been separated into reactive removal and stepwise vibrational deexcitation, and the rate constants given in Table 2 are for the sum of these processes.

reaction (1) has indicated that reactive removal of $v = 1$ and 2 comprises 38 and 45% of total removal [37], respectively, but with values of the total rates of removal in keeping with previous results as shown in Table 2. We correspondingly have analysed our data to include a reactive component by assuming that 40% of removal of all vibrational levels is by reaction, in keeping with the data suggested by the LIF study [37]. Fig. 4 illustrates that the fitting for the level most affected, $v = 1$ is now worse than for stepwise removal, and as shown in Table 2, the effect is largest on the returned value for $v = 1$, as would be expected. Our data analysed in this way now show a rate constant for the total removal of $v = 1$ which is considerably lower than the generally accepted value. We note that the rate constant for removal of OH($v = 0$) by CH_4, 6.3×10^{-15} cm^3 molecule^{-1} s^{-1} [1] would be enhanced by a factor of 33 for excitation of $v = 1$ if reactive removal constituted 38% of the measured removal rate. This is a surprisingly large value for excitation of what is essentially a spectator bond in a reaction where the activation energy (15 kJ mol^{-1}) is low in comparison with that for OH vibrational excitation, and the enhancement would be larger for $v = 2$. Yamasaki et al. [37] were unable to determine enhancement rates for levels above $v = 2$, but they note that their conclusions are inconsistent with previous measurements [2,9,10] of population ratios $v = 2/v = 3$, and they estimate a tentative value for this ratio of 0.78, i.e. a population inversion between these levels. Our data, which agree with previous TRFTIR measurements [2] and with QCT calculations [12], are unable to support such an inversion. We conclude that although we are unable to rule out a reactive enhancement of the chemical removal rate of OH by CH_4 as a result of vibrational excitation, our results are inconsistent with the enhancement being as large as that reported by Yamasaki et al. [37].

$O(^1D) + C_2H_6$

The reaction between $O(^1D)$ and ethane to form OH now only accounts for some 25% of the quantum yield of removal [38,39], in contrast to over 80% in the methane case [2–4], with the dominant reaction path leading to production of CH_3 radicals. The reaction can produce OH up to $v = 5$ for thermalised $O(^1D)$, and emission was readily observed from levels 1–4. Fig. 6 shows fundamental spectra taken at two times following reaction initiation with again the positions of the expected Q-branches marked.

What can be seen (but was absent from the corresponding reaction with CH_4) is a broad short lived emission underlying the resolved OH emission lines between 2700 and 3300 cm^{-1}: at the resolution used (5 cm^{-1}) the rotational structure of OH is expected to be almost completely resolved, as seen in Fig. 1, which is of a resolution of 4 cm^{-1}. The extra emission, which is in the C–H stretching region, was not identified: it was only partially removed by a cold gas filter containing ethane, and may arise from one of the reaction products CH_3, CH_2OH or C_2H_5, all of which have stretching frequencies in this region. The emission made extraction of vibrational populations in this spectral region difficult, and thus the overtone spectra (where C–H stretch overtones were not strong enough to interfere) were used for the higher vibrational levels. Fig. 7 and Table 3 show the resultant nascent populations, extracted in the same way as for $O(^1D)$ + methane, and are compared with two previous LIF

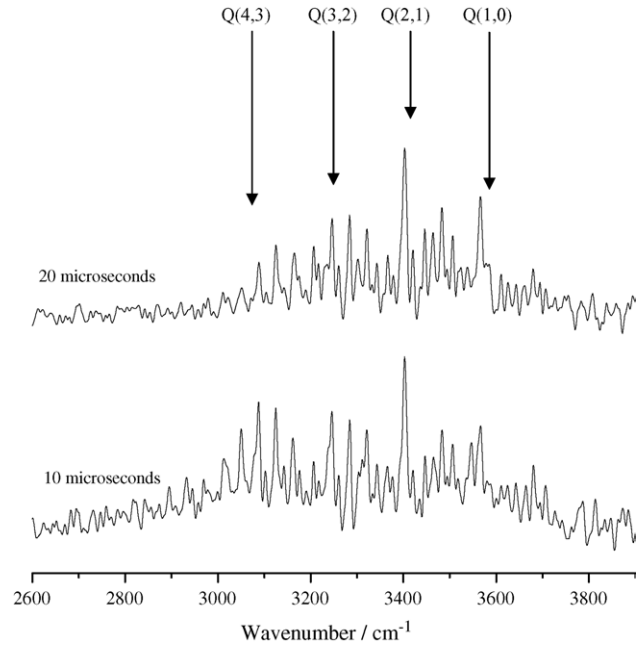

Fig. 6. OH($\Delta v = -1$) emission spectra at two times following reaction initiation from $O(^1D) + C_2H_6$: p(N_2O) = 63 m Torr, p(C_2H_6) = 126 m Torr, t = 10 μs (upper trace) and 20 μs (lower trace); resolution = 5 cm^{-1}.

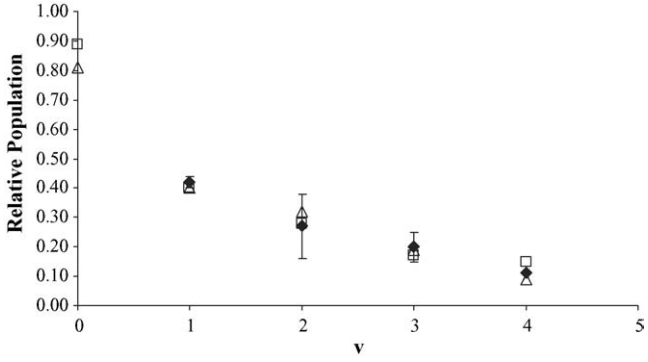

Fig. 7. OH nascent vibrational distributions from the reaction $O(^1D) + C_2H_6$ measured in this work (filled diamonds) and those of Park and Wiesenfeld [10] (squares) and Gonzalez et al. [40] (triangles).

studies, showing very good agreement between the two techniques.

The larger error bars than in the CH_4 data reflect the lower yield of OH, and also the more rapid rate of quenching observed

Table 3
OH nascent vibrational distributions from the reaction $O(^1D) + C_2H_6$, compared with previous measurements

v	Nascent population			Removal rate constants k (10^{-12} cm^3 molecules^{-1} s^{-1})
	This work	[10]	[40]	
0	–	0.89	0.81 ± 0.21	–
1	0.42 ± 0.02	0.40	0.40	1.18 ± 0.38
2	0.27 ± 0.11	0.28	0.32 ± 0.08	5.04 ± 0.63
3	0.20 ± 0.05	0.17	0.19 ± 0.04	9.44 ± 1.02
4	0.11 ± 0.06	0.15	0.09 ± 0.02	15.1 ± 3.96

The final column also shows rate constants k for relaxation of OH(v) by C_2H_6. Errors are shown as ±1σ. Populations are summed to unity for $v > 0$.

(see below). The mechanism again appears to be insertion into the C–H bond, but theoretical calculations based upon a mass corrected $O(^1D) + CH_4$ surface [40] have indicated a small proportion of collisions leading to abstraction.

Time resolved populations were converted into rate constants for vibrational relaxation, with the assumption of stepwise excitation as for the $OH(v) + CH_4$ case above. The reaction of OH with C_2H_6 has a room temperature rate constant of 2.5×10^{-13} cm^3 molecule^{-1} s^{-1} [1], considerably faster than that for CH_4 [1], and although in the treatment of the data we neglect chemical removal, the validity of this approach is perhaps more questionable than in the methane case. We note that calculations of the effect of vibrational excitation on the reaction rate however suggest that it is negligible [41]. No previous measurements of $OH(v)$ quenching by ethane appear to exist: we note that the data, also given in Table 3, show larger rate constants with a more pronounced increase with v than for the methane case. Both ν_5 and ν_{10} ir active modes in ethane occur near 3000 cm^{-1} and are available for energy transfer.

4. Reactions of CH_nF_{4-n}

Emission from the fundamental transitions ($\Delta v = -1$) of OH and HF formed in the reaction of $O(^1D)$ with CH_nF_{4-n} should occur in the region near 3600 cm^{-1}. The largest ratio of OH to HF production is expected in the reaction of CH_3F, where the quantum yields are in the ratio 1:1 [17], but the high value of the HF transition moment compared with that of OH means that the ratio of emission from OH to that of HF is expected to be approximately 1:10 [21,42]. Spectra were taken at 7 cm^{-1} resolution in order to separate the individual OH and HF transitions.

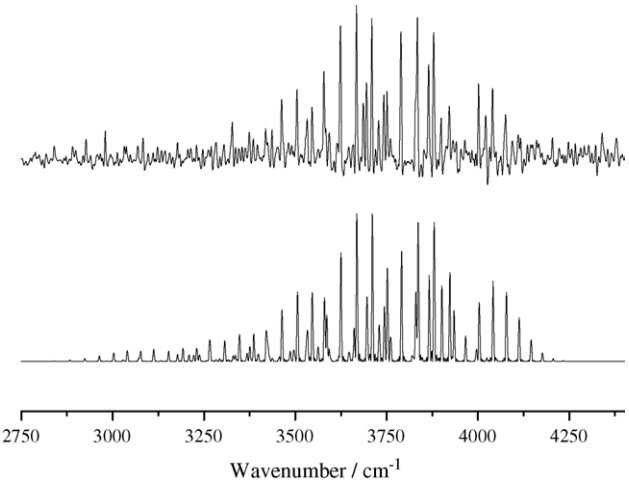

Fig. 8. HF($\Delta v = -1$) emission spectrum (upper trace) from $O(^1D) + CFH_3F$: $p(N_2O) = 27$ m Torr, $p(CH_3F) = 55$ m Torr, $t = 20$ μs. Also shown is the HF($\Delta v = -1$) simulation (lower trace).

The OH emission was too weak for its initial distribution to be successfully analysed, and the vibration–rotation lines were sufficiently separated from those of HF to ensure that they did not interfere with the analysis of the HF populations. Fig. 8 shows an example of an observed spectrum together with a fit to rotationally thermalised HF populations, with levels from $v = 1$–6 observed.

Extraction of populations were carried out in the same way as described for OH, with nascent distributions and rate constants for relaxation with the parent fluorocarbons CH_3F, CH_2F_2 and CHF_3 extracted for the six vibrational levels observed. The nascent distributions are presented in Table 4, and rate constants

Table 4
Nascent HF vibrational distributions measured for the $O(^1D)$ reactions with CH_3F, CH_2F_2 and CHF_3 reactions, and compared with previous data

v	CH_3F (this work)	CH_2F_2 (this work)	CHF_3 (this work)	CH_3F [11]	CH_2F_2 [11]	CHF_3 [6]	CHF_3 [11]
0	–	–	–	0.39	0.29	–	0.31
1	0.29 ± 0.02	0.26 ± 0.06	0.24 ± 0.03	0.34 ± 0.02	0.29 ± 0.01	0.25	0.29 ± 0.02
2	0.24 ± 0.05	0.23 ± 0.03	0.24 ± 0.04	0.25 ± 0.03	0.29 ± 0.03	0.21	0.24 ± 0.02
3	0.22 ± 0.05	0.22 ± 0.05	0.20 ± 0.03	<0.16	< 0.13	0.18	<0.15
4	0.13 ± 0.05	0.16 ± 0.02	0.14 ± 0.05	–	–	0.19	–
5	0.07 ± 0.03	0.08 ± 0.04	0.10 ± 0.02	–	–	0.12	–
6	0.04 ± 0.03	0.03 ± 0.02	0.09 ± 0.02	–	–	0.05	–

Errors are shown as ±1σ. The present data and those of [6] are summed to unity. For the data of [11], where only the first three of the vibrationally excited levels were measured, the populations have been summed to the same values as those for levels 1–3 in the present data.

Table 5
Vibrational quenching rate constants k_v in units of 10^{-11} cm^3 molecule^{-1} s^{-1} with a variety of collision partners

v	CH_3F (this work)	CH_2F_2 (this work)	CHF_3 (this work)	CF_4 [46]	CH_4 [46]	CH_4 [47]	CH_4 [48]	CH_4 [49]	CH_4 [50]
1	0.85 ± 0.13	0.31 ± 0.12	0.13 ± 0.03	0.07	4.0	–	–	–	0.07
2	1.92 ± 0.23	0.68 ± 0.17	0.26 ± 0.06	0.13	13.0	–	–	–	0.18
3	3.89 ± 0.72	1.45 ± 0.21	0.87 ± 0.14	0.38	16.0	1.45	1.8	–	0.47
4	5.02 ± 2.56	2.34 ± 0.77	1.17 ± 0.17	–	–	4.56	4.7	–	1.3
5	8.71 ± 0.91	4.11 ± 1.53	1.92 ± 0.29	–	–	12.1	–	10.0	3.0
6	9.00 ± 4.12	5.51 ± 0.90	–	–	–	–	–	14.0	4.8

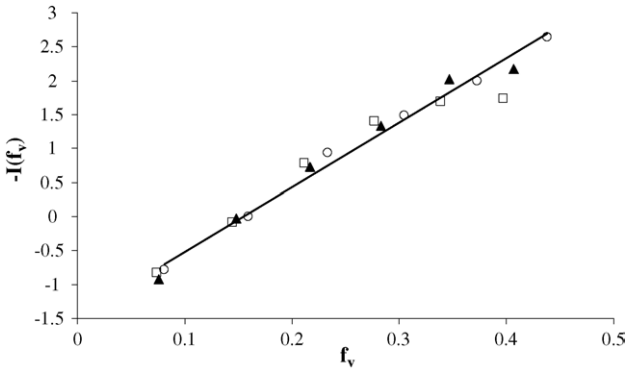

Fig. 9. Surprisal plot for the HF vibrational distributions formed in the O(^{1}D) reactions with CH_3F (circles), CH_2F_2 (squares) and CHF_3 (filled triangles). Prior distributions, $P^0(v)$, were calculated as given in Refs. [43,44] and the surprisal, $I(f_v) = -\ln[P(v)/P^0(v)]$ where $P(v)$ is the experimental probability of HF formation in level v. The positive slope of the plot of $-I(f_v)$ against f_v for the three fluorinated methanes indicates a greater than statistical partitioning of vibrational energy in HF, with the single straight line consistent with a similar mechanism for the O(^{1}D) reaction with the three fluorocarbons.

for vibrational relaxation are presented in Table 5 together with data from previous investigations.

The most striking observation of the nascent population data is that for all three reactions the distributions are very similar, and (with the exception of the equal populations of $v = 1$ and 2 for CHF_3) show a monotonic decrease of population with increasing v. Previous measurements on the CHF_3 reaction by Aker et al. [6] using the same TRFTIR technique but with O(^{1}D) formed by photolysis of ozone are in good agreement with present data (although we do not see the reported population inversion between $v = 3$ and 4, attributed to the formation of CF_2O in two different electronic states [6]). The more limited sets of measurements on CH_3F, CH_2F_2 and CHF_3 carried out for levels $v = 1$–3 by laser gain measurements also show the same trends [11]. Fig. 9 shows a surprisal plot [43,44] calculated with the rigid rotor harmonic oscillator approximation for the three reactions, indicating that the measured vibrational populations are hotter than those expected statistically, and are virtually the same for each process.

The results suggest that a mechanism involving insertion of O(^{1}D) into a C–H or C–F bond and redissociation on a time scale which does not result in complete randomisation of the available energy but is long enough to result in forward/backward scattering as observed for the O(^{1}D) + CFH_3 reaction [45].

Table 5 shows that rate constants for quenching of HF with the three fluorinated methanes used in this study demonstrate the expected increase with v, and for a given v are seen to increase with increasing H atom content, matching the increase in the number of ir active modes near 3000 cm^{-1} as F is replaced by H.

Previously measured rate constants for quenching by CF_4 [46] are slower than those reported here, in agreement with this trend, but for quenching by CH_4 the data are less clear-cut because of the range of values reported in the literature [46–50].

Finally we comment on a clear feature observed in all the spectra (including experiments carried out with CF_4), namely strong emission from the infrared active modes of the parent molecule in the 1100–1400 cm^{-1} region. The quenching process

$$O(^1D) + CH_nF_{4-n} \rightarrow CH_nF_{4-n} + O(^3P) \quad (6)$$

is thought to increase in quantum yield as the F atom content in the fluorocarbon increases [5,7] and it was hoped that emission from the vibrationally excited fluorinated methane might give information on the efficiency of energy transfer from O(^{1}D) to the parent molecule in process (6). However, both the rise time (too slow) and the intensity of the emission (too large) were inconsistent with process (6) being responsible in all systems studied, and it was concluded that vibrational excitation in the fluorocarbon appears to come from energy transfer either from vibrationally excited N_2O or from its precursor (vibrationally excited N_2) [19]. N_2O emission in the $\Delta v_3 = -1$ bands was reduced in intensity and increased in removal rate on addition of fluorocarbon. Experiments carried out with CF_4 (where chemical removal does not take place) showed substantial emission from vibrationally excited CF_4, but again its origin was inconsistent with the O(^{1}D) quenching mechanism. We are thus unable to verify the quantum yields of energy transfer in process (6) to vibrational levels of CH_nF_{4-n}.

5. Conclusions

Time resolved FTIR emission has been used to study the dynamics and kinetics of O(^{1}D) reactions with hydrocarbons. The technique allows observation of all vibrationally excited levels simultaneously, and although it is not as sensitive as laser detection methods such as LIF it does not require significant corrections of the observed signals over differing experimental conditions in order to extract nascent vibrational populations. For reaction of O(^{1}D) with methane, the vibrational populations of $v = 1$–4 show a population inversion between the lowest two levels, and are in excellent agreement with previous observations [2,9,10] and with QCT calculations [12]. Reaction with ethane does not show such an inversion: in this case measurements on the first overtone emission were needed in order to avoid overlap of OH emission with that from C–H stretching frequencies. Quenching rates were measured and discussed in terms of stepwise excitation versus chemical reaction, with the conclusion that the former dominates in collisions of OH(v) with both hydrocarbons. For the reactions with CH_3F, CH_2F_2 and CHF_3, HF was observed as the major emitting reaction product, and nascent vibrational distributions measured for $v = 1$–6 show distinct similarities, and a higher than statistical fraction of the available energy appearing in vibration. Stepwise relaxation rate constants of HF(v) with the parent fluorocarbons increased in magnitude with H atom content of the molecule.

Acknowledgements

The research was funded under the EPSRC Portfolio scheme “Laser”. MM thanks Bruker UK for partial financial support.

References

[1] W.B. DeMore, S.P. Sander, D.M. Golden, R.F. Hampson, M.J. Kurylo, C.J. Howard, A.R. Ravishankara, C.E. Kolb, M.J. Molina, Chemical kinetics and photochemical data for use in stratospheric modeling, evaluation number 12, 1997.
[2] P.M. Aker, J.J.A. O'Brien, J.J. Sloan, J. Chem. Phys. 84 (1986) 745.
[3] S. Satyapal, J. Park, R. Bersohn, B. Katz, J. Chem. Phys. 91 (1989) 6873.
[4] W. Hack, H. Thiesemann, J. Phys. Chem. 99 (1995) 17364.
[5] A.P. Force, J.R. Wiesenfeld, J. Phys. Chem. 85 (1981) 782.
[6] P.M. Aker, B.I. Niefer, J.J. Sloan, J. Chem. Phys. 87 (1987) 203.
[7] A.M. Schmoltner, R.K. Talukdar, R.F. Warren, A. Mellouki, L. Goldfarb, T. Gierczak, S.A. McKeen, A.R. Ravishankara, J. Phys. Chem. 97 (1993) 8976.
[8] J. Shu, J.J. Lin, Y.T. Lee, X. Yang, J. Chem. Phys. 113 (2000) 9678.
[9] S.G. Cheskis, A.A. Iogansen, P.V. Kulakov, I.Yu. Razuvaev, O.M. Sarkisov, A.A. Titov, Chem. Phys. Lett. 155 (1989) 37.
[10] C.R. Park, J.R. Wiesenfeld, J. Chem. Phys. 95 (1991) 8166.
[11] T.L. Burks, M.C. Lin, Int. J. Chem. Kinet. 13 (1981) 977.
[12] M. Gonzalez, M.P. Puyuelo, J. Hernando, R. Sayos, P.A. Enriquez, J. Guallar, I. Banos, J. Phys. Chem. 104 (2000) 521.
[13] G.A. Raiche, J.B. Jeffries, K.J. Rensberger, D.R. Crosley, J. Chem. Phys. 92 (1990) 7258.
[14] E. Silvente, R.C. Richter, A.J. Hynes, J. Chem. Soc. Faraday Trans. 93 (1997) 2821.
[15] M. Kneba, J. Wolfrum, Annu. Rev. Phys. Chem. 31 (1980) 47.
[16] K.J. Rensberger, J.B. Jeffries, D.R. Crosley, J. Chem. Phys. 90 (1989) 2174.
[17] T.L. Burks, M.C. Lin, Chem. Phys. 33 (1978) 327.
[18] C. Morrell, C. Breheny, V. Haverd, A. Cawley, G. Hancock, J. Chem. Phys. 117 (2002) 11121.
[19] G. Hancock, V. Haverd, Phys. Chem. Chem. Phys. 5 (2003) 2369.
[20] J.J. Lin, S. Harich, Y.T. Lee, X. Yang, 110 (1999) 10821.
[21] D.N. Turnbull, R.P. Lowe, Planet. Space Sci. 37 (1989) 723.
[22] G. Hancock, M. Morrison, Mol. Phys. 103 (2005) 1727.
[23] P. Felder, B.M. Haas, J.R. Huber, Chem. Phys. Lett. 186 (1991) 177.
[24] Y. Matsumi, S.M. Shamsuddin, Y. Sato, M. Kawasaki, J. Chem. Phys. 101 (1994) 9610.
[25] P.H. Wine, A.R. Ravishankara, Chem. Phys. Lett. 77 (1981) 103.
[26] M. Gonzalez, J. Hernando, I. Banos, R. Sayos, J. Chem. Phys. 111 (1999) 8913.
[27] M. Gonzalez, J. Hernando, I. Banos, R. Sayos, J. Chem. Phys. 113 (2000) 6748.
[28] A.C. Luntz, J. Chem. Phys. 73 (1980) 1143.
[29] R.D. van Zee, J.C. Stephenson, M.P. Casassa, Chem. Phys. Lett. 223 (1994) 167.
[30] H.G. Yu, J.T. Muckerman, J. Phys. Chem. A 108 (2004) 8615.
[31] W.B. DeMore, O.F. Raper, J. Chem. Phys. 46 (1967) 2500.
[32] M. Brouard, S. Duxon, P.A. Enriquez, J.P. Simons, J. Chem. Soc. Faraday Trans. 89 (1993) 1435.
[33] M. Brouard, S.P. Duxon, J.P. Simons, Isr. J. Chem. 34 (1994) 67.
[34] M. Brouard, H.M. Lambert, C.L. Russell, J. Short, J.P. Simons, Faraday Discuss. 102 (1995) 179.
[35] C.C. Miller, R.D. van Zee, J.C. Stephenson, J. Chem. Phys. 114 (2001) 1214.
[36] G.P. Glass, H. Endo, B.K. Chaturvedi, J. Chem. Phys. 77 (1982) 5450.
[37] K. Yamasaki, A. Watanabe, T. Kakuda, N. Ichikawa, I. Tokue, J. Phys. Chem. A 103 (1999) 451.
[38] J. Shu, J.J. Lin, Y.T. Lee, X. Yang, J. Chem. Phys. 114 (2001) 4.
[39] J. Shu, J.J. Lin, Y.T. Lee, X. Yang, J. Chem. Phys. 115 (2001) 849.
[40] M. Gonzalez, M.P. Puyuelo, J. Hernando, R. Sayos, P.A. Enriquez, J. Guallar, J. Phys. Chem. A 105 (2001) 9384.
[41] S. Sekak, M.G. Corey, R.J. Bartlett, A. Sabljia, J. Phys. Chem. A 103 (1999) 11394.
[42] W.T. Zemke, W.C. Stwalley, S.R. Langhoff, G.L. Valderrama, M.J. Berry, J. Chem. Phys. 95 (1991) 7846.
[43] R.D. Levine, R.B Bernstein, Molecular Reaction Dynamics and Chemical Reactivity, OUP, 1987.
[44] J.T. Muckerman, J. Phys. Chem. 93 (1989) 179.
[45] J. Shu, J.J. Lin, Y.T. Lee, X. Yang, J. Chem. Phys. 113 (2000) 9678.
[46] M.A. Kwok, N. Cohen, J. Chem. Phys. 61 (1974) 5221.
[47] G.M. Jurisch, D.R. Ritter, F.F. Crim, J. Chem. Phys. 80 (1984) 4097.
[48] J.D. Lambert, G.M. Jurisch, F.F. Crim, J. Chem. Phys. Lett. 71 (1980) 258.
[49] L.S. Dzelkalns, F. Kaufman, J. Chem. Phys. 77 (1982) 3508.
[50] P.R. Poole, I.W.M. Smith, J. Chem. Soc. Faraday Trans. 73 (1977) 1447.